| AD NUMBER |
| --- |
| **AD460971** |
| LIMITATION CHANGES |
| TO:<br>**Approved for public release; distribution is unlimited.** |
| FROM:<br>**Distribution authorized to U.S. Gov't. agencies and their contractors; Administrative/Operational Use; JUN 1964. Other requests shall be referred to Air Force Space Systems Division, Los Angeles AFB, CA.** |
| AUTHORITY |
| **samso ltr, 11 sep 1968** |

REPORT NO. N-115257
TOR-269(4540-80)-3

# Infrared Horizon Sensor Accuracy in the Atmospheric Absorption Bands



JUNE 1964



*Prepared by* M. D. EARLE
*Electrical and Optical Department*
*Sensing and Information Systems Subdivision*
*Electronics Division*

*Prepared for* COMMANDER SPACE SYSTEMS DIVISION
AIR FORCE SYSTEMS COMMAND
LOS ANGELES AIR FORCE STATION
*Los Angeles, California*

EL SEGUNDO TECHNICAL OPERATIONS • AEROSPACE CORPORATION
CONTRACT NO. AF 04(695)-269

14 Report No.
TOR-269(4540-80)-3

5 Aerospace Corp., El Segundo, Calif.

6 INFRARED HORIZON SENSOR ACCURACY IN THE
ATMOSPHERIC ABSORPTION BANDS,

[redacted]

10 by M. D. Earle,
~~Electrical and Optical Department~~
~~Sensing and Information Systems Subdivision~~
~~Electronics Division~~

15 Contract [redacted] AF 04(695)-269

3

11 June 1964,

Prepared for
COMMANDER SPACE SYSTEMS DIVISION
AIR FORCE SYSTEMS COMMAND
LOS ANGELES AIR FORCE STATION
Los Angeles, California

12795

Report No.
TOR-269(4540-80)-3

INFRARED HORIZON SENSOR ACCURACY IN THE ATMOSPHERIC ABSORPTION BANDS

Prepared by

M. D. Earle

M. D. Earle
Manager, Infrared Section

Approved by

A. G. Nash

A. G. Nash, Head
Electrical and Optical Department

A. G. Nash for L. H.

L. Hirschl, Director
Sensing and Information Systems Subdivision

## FIGURES


1. Apparent Earth Cloud Temperatures . . . . . . . . . . . . . . . . . . 2

2. Space-Earth Pulse . . . . . . . . . . . . . . . . . . . . . . . . . . 4

3. Atmospheric Radiance Profile . . . . . . . . . . . . . . . . . . . . 7

4. Atmospheric Models A, B, C, and D (Radiance Vs Altitude, 14.29 to 16.0 Microns). . . . . . . . . . . . . . . . . . . . . . . . . . 11

5. Atmospheric Models E, F, G, and H (Radiance Vs Altitude, 14.29 to 16.0 Microns). . . . . . . . . . . . . . . . . . . . . . . . . . 12

6. Atmospheric Models A, B, C, and D (Radiance Vs Altitude, 12.30 to 14.80 Microns) . . . . . . . . . . . . . . . . . . . . . . . . 16

7. Atmospheric Models A, B, C, and D (Radiance Vs Altitude, 16.0 to 18.2 Microns). . . . . . . . . . . . . . . . . . . . . . . . . . 17

8. Atmospheric Model A (Radiance and Radiance Difference Vs Altitude, 14.29 to 16.0 and 16.0 to 17.4 Microns) . . . . . . . . . . . 19

9. Atmospheric Model C (Radiance and Radiance Difference Vs Altitude, 14.29 to 16.0 and 16.0 to 17.4 Microns) . . . . . . . . . . . 21

10. Atmospheric Model A (Radiance and Radiance Difference Vs Altitude, 14.29 to 16.0 and 12.85 to 14.29 Microns). . . . . . . . . . 23

11. Atmospheric Model C (Radiance and Radiance Difference Vs Altitude, 14.29 to 16.0 and 12.85 to 14.29 Microns). . . . . . . . . . 24

12. Atmospheric Models A, B, C, and D (Radiance Vs Altitude, 28.6 to 40.0 Microns) . . . . . . . . . . . . . . . . . . . . . . . . . 25

13. Atmospheric Models E, F, G, and H (Radiance Vs Altitude, 28.6 to 40.0 Microns) . . . . . . . . . . . . . . . . . . . . . . . . . 26

## TABLES

1. Atmospheric Models . . . . . . . . . . 6

2. Analysis of Horizon Radiance Data for 14.29 to 16.0 Micron Spectral Region . . . . . . . . . . 13

3. "Two-Color" Horizon Sensing Technique . . . . . . . . . . 20

4. Analysis of Horizon Radiance Data for 28.6 to 40.0 Micron Spectral Region . . . . . . . . . . 27

CONTENTS

ABSTRACT . . . . . . . . . . vi

I. INTRODUCTION . . . . . . . . . . 1

II. THE 14.29 TO 16.0 MICRON REGION . . . . . . . . . . 10

III. SPECTRAL REGIONS ADJACENT TO THE $CO_2$ ABSORPTION BAND . . . . . . . . . . 15

IV. "TWO COLOR" HORIZON SENSING TECHNIQUES . . . . . . . . . . 18

V. THE LONG WAVELENGTH ROTATIONAL ABSORPTION BAND OF WATER VAPOR . . . . . . . . . . 27

VI. CONCLUSIONS . . . . . . . . . . 29

REFERENCES . . . . . . . . . . 31

# ABSTRACT

An analysis has been made of atmospheric radiance data which ~~was~~ were computed by the Weather Bureau based on a variety of atmospheric models. Narrow spectral regions, located within the carbon dioxide absorption band centered at 15 microns, have been considered. It is shown that a spectral band approximately 1.7 microns wide centered very close to the absorption band shows promise, when the data is properly processed, of providing 1σ horizon sensor accuracies of about 0.05 degrees. A "two color" technique involving the use of two spectral regions in the vicinity of the $CO_2$ absorption band is discussed.

The possibility of using the 28.6 to 40.0 micron spectral region within the broad rotational water vapor absorption band is also considered.

# I. INTRODUCTION

Infrared horizon sensor technology has now reached the point where the instrumental errors are far smaller than those which result from uncertainties and variations in the radiation characteristics of the earth's horizon. For this reason the question of the optimum spectral band in which to operate becomes very important.

Earlier horizon sensors operated in a very broad region of the infrared spectrum, extending from approximately 2 microns to about 18 or 20 microns. Since germanium is a useful optical material in this region, the long wavelength cutoff was usually established by the germanium optics at about 18 or 20 microns, depending on the length of the optical path in the germanium.

In addition to several atmospheric absorption bands, the 2 to 18 micron spectral region also contains the broad atmospheric "window" between 8 and 13 microns. Since the atmosphere is quite transparent in this region, the radiation profile of the earth's horizon can be seriously affected by meteorological conditions. In clear weather the earth itself will be the source of radiation on which the horizon sensor operates. In overcast weather the effective source of radiation may be a layer of high clouds, whose temperature is considerably lower than that of the earth. An even more serious situation, and one which often occurs, is the inclusion of earth and high cold clouds in different portions of the same scan. Figure 1 gives a comparison of the approximate magnitude of the temperature difference between earth and clouds. These plots show samples of data obtained by the Barnes Engineering Company (Ref. 1) using a calibrated conical scan horizon sensor with a spectral bandpass of 2 to 18 microns mounted on a Mercury vehicle (Mercury Mission MA-5, November 29, 1961). It can be seen that the apparent temperature of the earth is approximately 250°to 260°K, while the apparent temperature of some clouds is as low as 170°K.

In a conical scan horizon sensor system in which attitude information is obtained by comparing the position of the center of the pulse generated as the

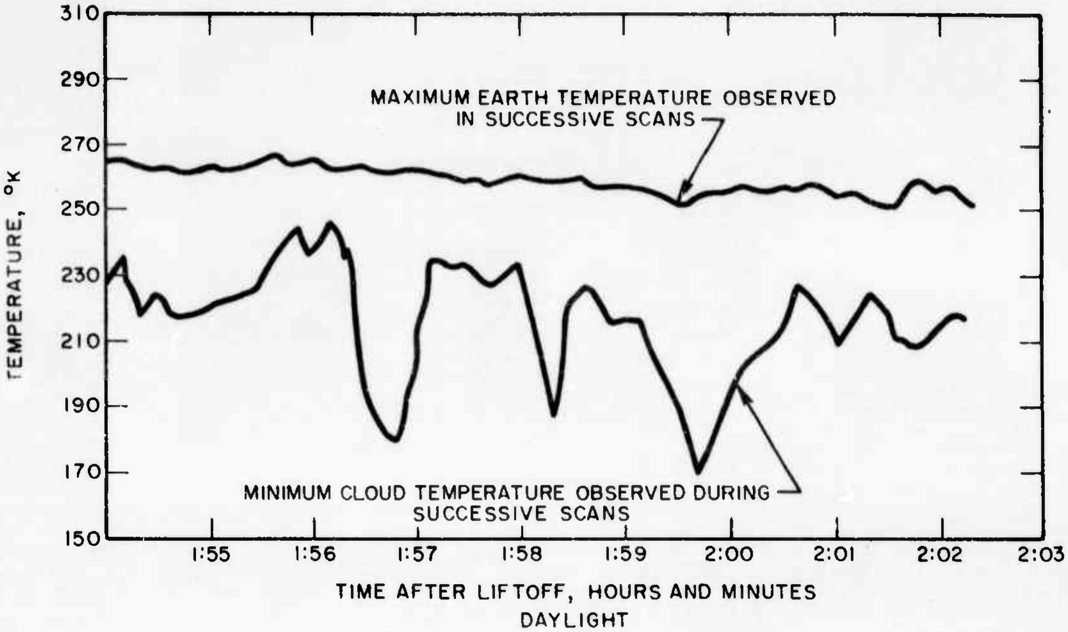


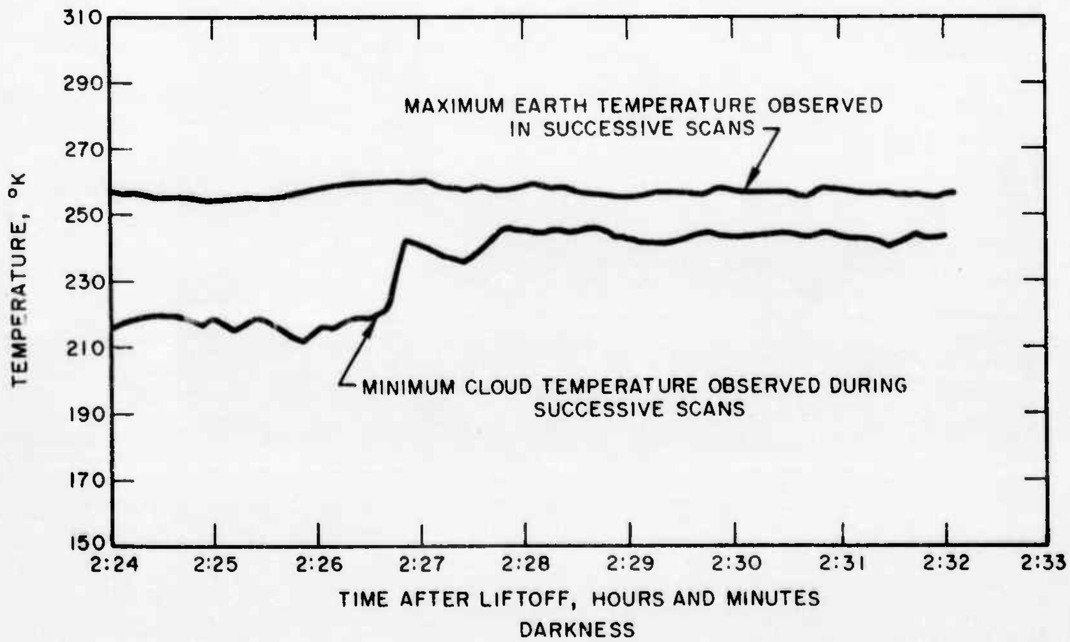


Figure 1. Apparent Earth Cloud Temperatures

scan crosses the earth, with a fixed reference, the presence of a cloud in a portion of the scan can cause serious errors. This is illustrated in Figure 2. The cloud problem can be partially avoided by clipping the signal below the level at which most of the cloud dips occur; however, if this clipping level is made too low, serious signal-to-noise problems will develop.

An edge tracking system which scans vertically across the horizon, locking onto the radiance gradient in accordance with some predetermined criterion, will also be seriously affected by the presence of clouds if the system spectral bandwidth includes the atmospheric window region. The altitude of the apparent horizon above the earth will vary with meteorological conditions and serious errors will result.

Since it would be preferable to avoid "seeing" the clouds altogether, the chosen spectral region for horizon sensor operation should not include the 8 to 13 micron "window" or any significantly large portions of it. Thus the use of a reasonably narrow spectral region centered at one of the atmospheric absorption bands is indicated. Then, hopefully, the atmosphere would become opaque at an altitude above that at which clouds are usually found.

There is an atmospheric absorption band located at approximately 2.7 microns which is caused by water vapor and carbon dioxide. There are also absorption bands at 4.3 microns and 6.3 microns because of the presence of carbon dioxide and water vapor respectively. At 15 microns there is a strong absorption band caused by carbon dioxide. There is also a very broad water vapor absorption band located in the vicinity of 20 to 40 microns.

Several investigations have clearly indicated the superiority of the two latter absorption bands over the three former (Refs. 2 through 5). In particular, the $CO_2$ absorption band at 15 microns shows great promise for horizon sensing purposes. There are two principal reasons for this: One is that carbon dioxide has a very uniform distribution throughout the atmosphere, having a concentration by volume of approximately 0.031 percent. The other important reason is that the peak of the thermal radiation from the earth occurs in the vicinity of 15 microns. Since a horizon sensor operating in an absorption band does not track the true earth horizon, but rather a point on

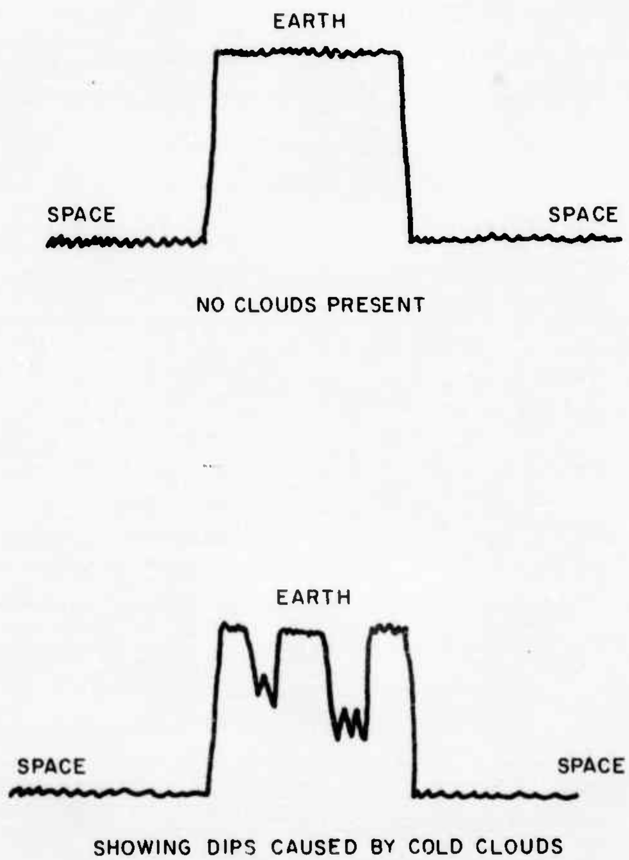


Figure 2. Space-Earth Pulse

the horizon radiance curve at a considerable altitude, it is very important that the absorbing gas be uniformly distributed so that accuracy and reproducibility may be achieved.

The 2.7 micron, 4.3 micron, and 6.3 micron absorption bands are not useful for horizon sensing because of the small amount of thermal radiation emitted by the earth's atmosphere in these spectral regions. Also, particularly in the 2.7 micron band, there is a problem with scattered sunlight which will cause objectionable variations in radiance between day and night.

Although the water vapor absorption band near 35 microns shows some promise, it is less desirable for use in horizon sensing than the 15 micron $CO_2$ absorption band because of the nonuniformity of the distribution of water vapor in the atmosphere.

A report published by the Weather Bureau (Ref. 5) contains the results of atmospheric radiance calculations which were made from seven atmospheric models measured at widely separated points in the northern hemisphere. In addition the ARDC standard atmosphere of 1959 is included as one of the atmospheric models. The atmospheric models used and the locations at which they were measured, together with the dates and weather conditions are shown in Table 1.

In general it might be agreed that eight samples would not be a sufficient number from which to draw conclusions of a statistical nature. In the work considered here, however, the atmospheric models were selected to represent rather extreme locations and weather conditions with a variety of conditions between the extremes. For these reasons it is felt that a careful analysis of the data calculated from these models will provide a worthwhile estimate of the magnitude of the errors produced in a horizon sensor system by variations and uncertainties in the atmospheric radiance profile.

The above mentioned report presents detailed data on the atmospheric radiance profile as a function of wavenumber in $cm^{-1}$ and closest approach of the line of sight to the earth in kilometers (designated as "h" in Figure 3). The data extends from 2330 $cm^{-1}$ to 12.5 $cm^{-1}$ (4.28 microns to 800 microns).

Table 1. Atmospheric Models

| Designation | Location | Weather Conditions | Total Water VAPOR (grams/cm$^3$) | Total OZONE Content (cm-atmospheres) | Date | Time of Day (GMT hrs) |
|---|---|---|---|---|---|---|
| A | (ARDC. Standard) | Clear | 1.334 | 0.435 | 1959 | |
| B | Albuquerque, New Mexico | Clear | 1.363 | 0.289 | 7-11-58 | 0000 |
| C | Ponope, Caroline Islands | Undercast at 100 mb pressure | 0.001 | 0.293 | 5-17-58 | 1200 |
| D | Resolute, Northwest Territory | Undercast at 400 mb pressure | 0.007 | 0.273 | 12-31-58 | 1200 |
| E | Isachsen, Northwest Territory | Clear | 0.265 | 0.255 | 9-29-58 | 1200 |
| F | Barter Island, Alaska | Clear | 0.117 | 0.273 | 1-1-58 | 1200 |
| G | Kindley, Bermuda | Clear | 5.078 | 0.255 | 8-1-58 | 1200 |
| H | Thule, Greenland | Clear | 0.159 | 0.254 | 10-20-58 | 0000 |

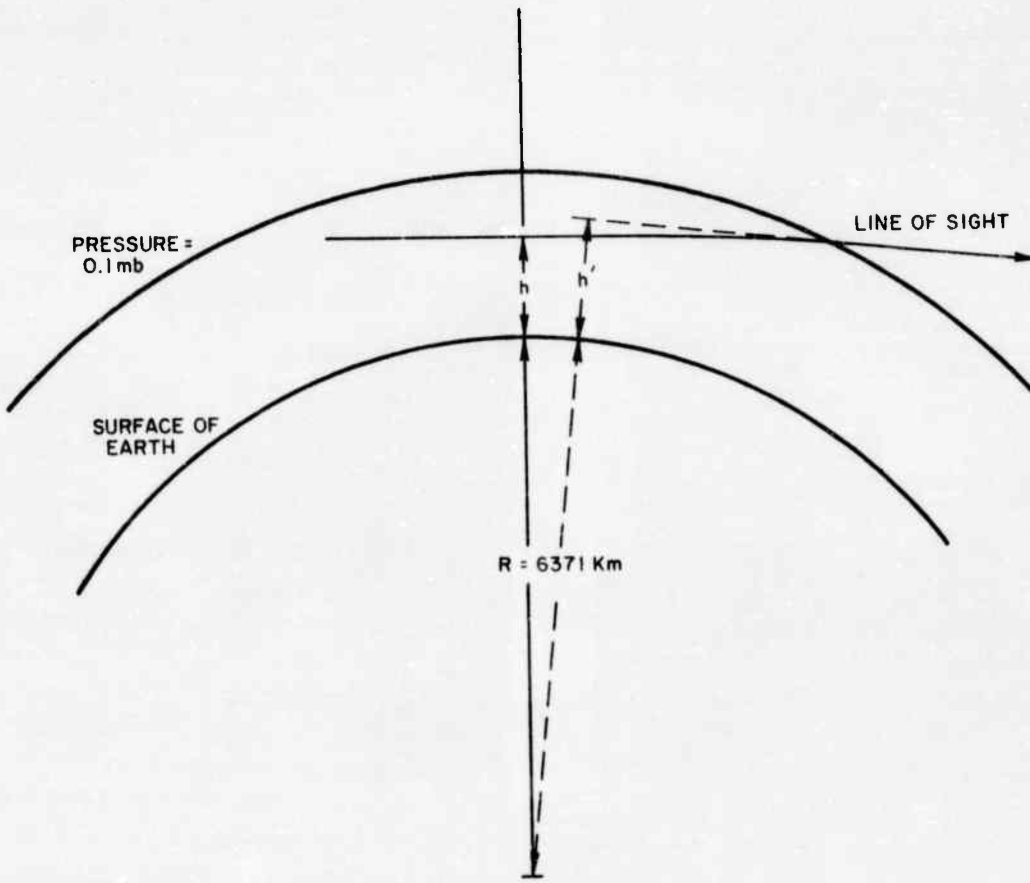


Figure 3. Atmospheric Radiance Profile

The Weather Bureau radiance values were computed by assuming that the earth's atmosphere was divided into 200 concentric layers, between sea level and the altitude where the pressure is 0.1 millibar. The spectrum from 4.28 microns to 800 microns was divided into 77 intervals. The radiance of each layer was computed using the data of a particular atmospheric model which shows temperature, pressure, and absorber concentration as a function of altitude. The radiance of each layer was multiplied by the transmission of the remaining layers above the one in question. These radiance values were then summed for each spectral interval and each value of h, making it possible to plot curves showing radiance as a function of "h" for any spectral region within the range investigated. In the original calculations, the refraction of the atmosphere was taken into consideration. Refraction causes the slant-path through the atmosphere to curve, increasing its length over that which would be used if a nonrefractive atmosphere were assumed.

In Figure 3, h is the actual distance of closest approach of the line of sight to the earth while h' is the apparent distance as seen from space. In the determination of errors in the angular position of the line of sight direction in space, the difference between h and h' is not significant, since the changes in the errors produced as a result of atmospheric refraction are small compared with the uncertainties in the errors themselves.

It is the purpose of this report to analyze in some detail the data for the spectral region near 15 microns contained in the Weather Bureau report, to ascertain the accuracy which may be expected of an edge tracking horizon sensor operating at this wavelength. Radiance versus altitude data for narrow spectral regions on either side of the center of the 15 micron absorption band are also shown. A comparison is made of the characteristics of these spectral bands with those of the band at the center of the absorption band. The results show that it is advantageous to operate as near as possible to the center of the band.

Curves are also shown of the radiance differences between two adjacent spectral regions plotted against the altitude h. It will be seen that these differences reach a maximum at a reasonably well defined value of h. The

possibility of using this technique for horizon sensing is discussed. In addition to the above, curves are presented showing atmospheric radiance in the 28.6 to 40.0 micron water vapor absorption spectral region. This region is shown to be inferior to the $CO_2$ absorption region for horizon sensing purposes.

## II. THE 14.29 TO 16.0 MICRON REGION

This spectral region is located very near the center of the $CO_2$ absorption band. The radiance values shown in Figures 4 and 5 were obtained by combining three of the spectral intervals shown in Reference 5. The radiances caused by these three narrow bands were combined to provide radiance of a realistic magnitude for the operation of horizon sensors.

Figure 4 shows the atmospheric radiance versus h within the spectral region 14.29 to 16.0 microns for atmospheric models A, B, C, and D. Figure 5 shows the same for atmospheric models E, F, G, and H.

It can readily be seen from the graphs that there is considerable variation in the absolute values of the curves. It can also be seen that if a threshold were set at a fixed value of radiance, and the value of h where the radiance reaches this value were arbitrarily defined as the horizon, considerable errors would result. For example, if the value $2 \times 10^{-4}$ watts $cm^{-2}$ $ster^{-1}$ were taken as the threshold, the differences in the corresponding values of h could be as large as 6.5 kilometers (between atmospheres B and D); on the other hand, if the horizon is defined as the value of h where the particular radiance curve reaches a certain fraction of its peak value, much higher accuracy can be obtained. This is equivalent to normalizing the atmospheric radiance curves to a common maximum value. Thus, in this method of processing, only the shape of the curves is of consequence. There appears to be much less variation in the shape of the horizon radiance profile than in its absolute value.

This would be a reasonably easy system to mechanize in an actual system, since it would only be necessary to measure the peak detector output signal at reasonably close intervals and then threshold the device at a predetermined fraction of this maximum signal. Another advantage of this system is that, since absolute values are no longer important, errors caused by slow changes in the responsitivity of the system would be minimized.

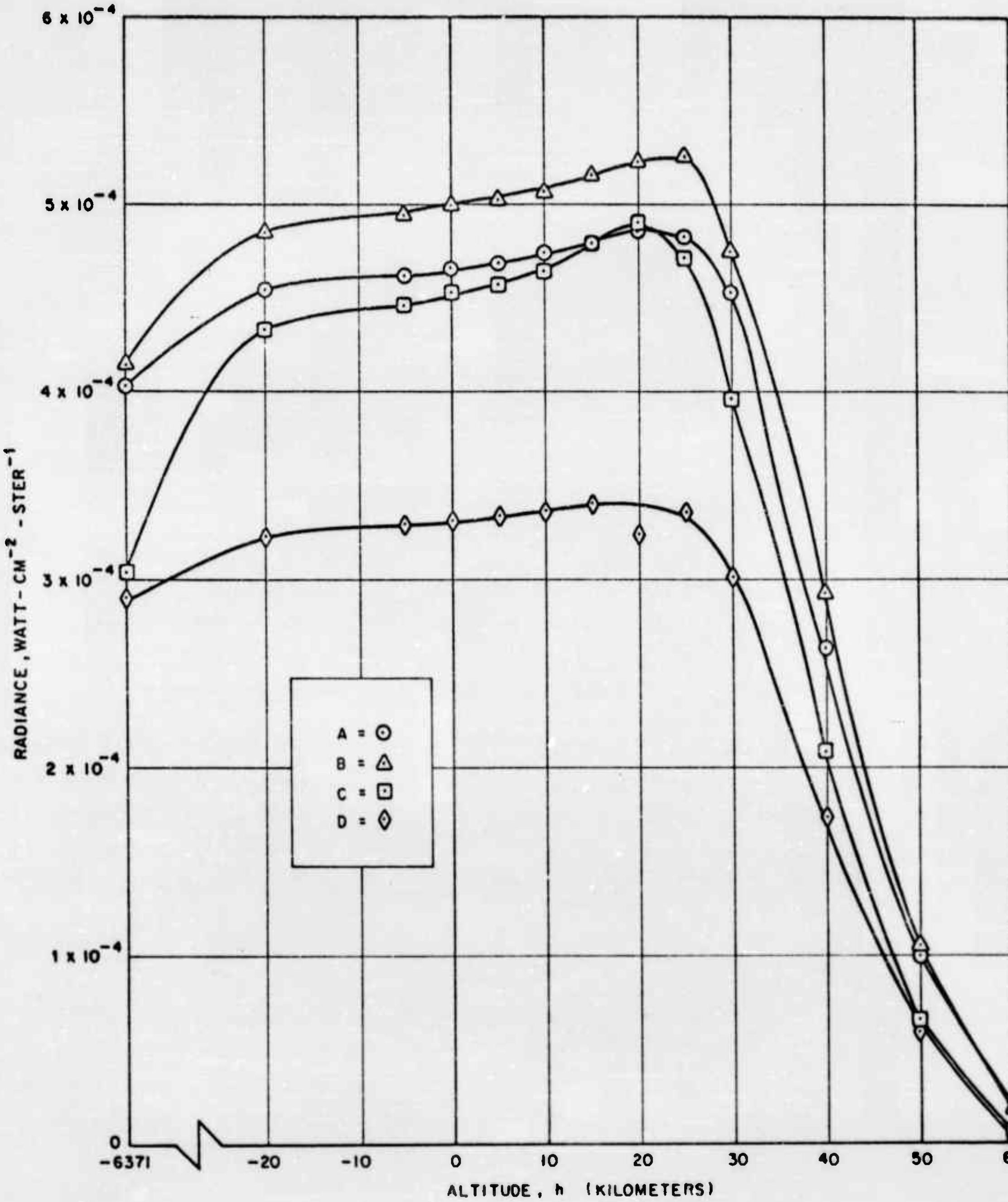


Figure 4. Atmospheric Models A, B, C, and D (Radiance Vs Altitude, 14.29 to 16.0 Microns)


Figure 5. Atmospheric Models E, F, G, and H (Radiance Vs Altitude, 14.29 to 16.0 Microns)

Table 2 shows the values of h in kilometers corresponding to various fractions (from 10 percent to 90 per cent) of the maximum radiance value for each atmospheric model. Column 9 gives the maximum difference for the models considered, while column 10 shows the standard deviation for the measurements of h corresponding to each percentage value.

Table 2. Analysis of Horizon Radiance Data for 14.29 to 16.0 Micron Spectral Region

| Atmospheric Model | 1 | 2 | 3 | 4 | 5 | 6 | 7 | 8 | 9 | 10 |
|---|---|---|---|---|---|---|---|---|---|---|
| Percent of Peak | A | B | C | D | E | F | G | H | Max. Diff. (km) | $\sigma$ (km) |
| 90 | 31.0 | 30.0 | 28.0 | 29.2 | 29.5 | 30.5 | 29.0 | 29.0 | 3.0 | 0.89 |
| 80 | 34.8 | 33.0 | 30.5 | 32.0 | 33.5 | 33.5 | 32.4 | 33.0 | 4.3 | 1.23 |
| 70 | 37.0 | 35.3 | 33.0 | 34.5 | 36.3 | 35.3 | 35.0 | 36.0 | 4.0 | 1.14 |
| 60 | 39.5 | 38.0 | 35.3 | 37.0 | 38.5 | 37.5 | 37.5 | 38.5 | 4.2 | 1.26 |
| 50 | 41.7 | 40.5 | 37.8 | 40.0 | 41.5 | 40.3 | 39.7 | 40.5 | 3.9 | 1.13 |
| 40 | 44.7 | 43.5 | 40.5 | 43.0 | 44.5 | 43.2 | 43.3 | 43.5 | 4.2 | 1.20 |
| 30 | 47.5 | 46.5 | 43.8 | 45.8 | 47.4 | 46.5 | 47.1 | 47.0 | 3.7 | 1.12 |
| 20 | 51.2 | 50.0 | 47.5 | 50.0 | 50.5 | 50.2 | 51.0 | 50.5 | 3.7 | 1.07 |
| 10 | 55.5 | 55.0 | 52.3 | 54.0 | 55.5 | 55.4 | 56.0 | 55.0 | 3.7 | 1.12 |

It would, of course, be desirable to have many more specific atmospheric model determinations from which to compute the standard deviation. But, as mentioned earlier, since the models were selected to represent extreme conditions as well as various conditions in between, they are assumed to be sufficiently valid samples to allow the computation of a standard deviation. Thus the computed standard deviations could be considered to be the $1\sigma$ error of a horizon sensor operating in the 14.29 to 16.0 micron region. The angular error to which this corresponds, depends, of course, on the altitude of the vehicle on which the horizon sensor is mounted.

The numbers in column 10 of Table 2 do not strongly suggest a particular fractional value of maximum radiance at which to operate; however, it appears that any fixed fractional value between 50 and 80 percent would be satisfactory. One would not want to operate at a very small fractional part of the maximum signal since this might introduce a signal-to-noise problem. On the other hand, if a value very near the peak were chosen, an additional uncertainty would be introduced by the flattening out of the radiance profile as the peak value is approached.

From an inspection of Table 2, it is seen that $1\sigma$ values of horizon uncertainties of about 0.9 to 1.3 kilometers can be expected.

If a space vehicle were at an altitude of 185 kilometers (100 nautical miles), the slant path to the earth's horizon would be about 1600 kilometers. Thus the angular $1\sigma$ error in the line of sight as determined by the horizon sensor would be 1.3/1600 radians, which is slightly less than 0.05 deg. As the altitude of the vehicle increases, the angular uncertainty is reduced in proportion.

## III. SPECTRAL REGIONS ADJACENT TO THE $CO_2$ ABSORPTION BAND

Figure 6 shows horizon radiance curves for the 12.30 to 14.80 micron spectral region for atmospheres A, B, C, and D. This spectral region is just to the short wavelength side of the center of the $CO_2$ absorption band. Figure 7 shows similar horizon radiance curves for the same four atmospheric models for the 16.0 to 18.2 micron spectral region, which is just to the long wavelength side of the $CO_2$ absorption band.

It can be seen from these curves that there is more variation in the shapes of the curves than is the case for the horizon radiance profiles in the 14.29 to 16.0 micron spectral region which is more nearly in the center of the $CO_2$ absorption band. Thus it is indicated that not only should a reasonably narrow band of radiation be used, but that it should be near the region of maximum absorption.

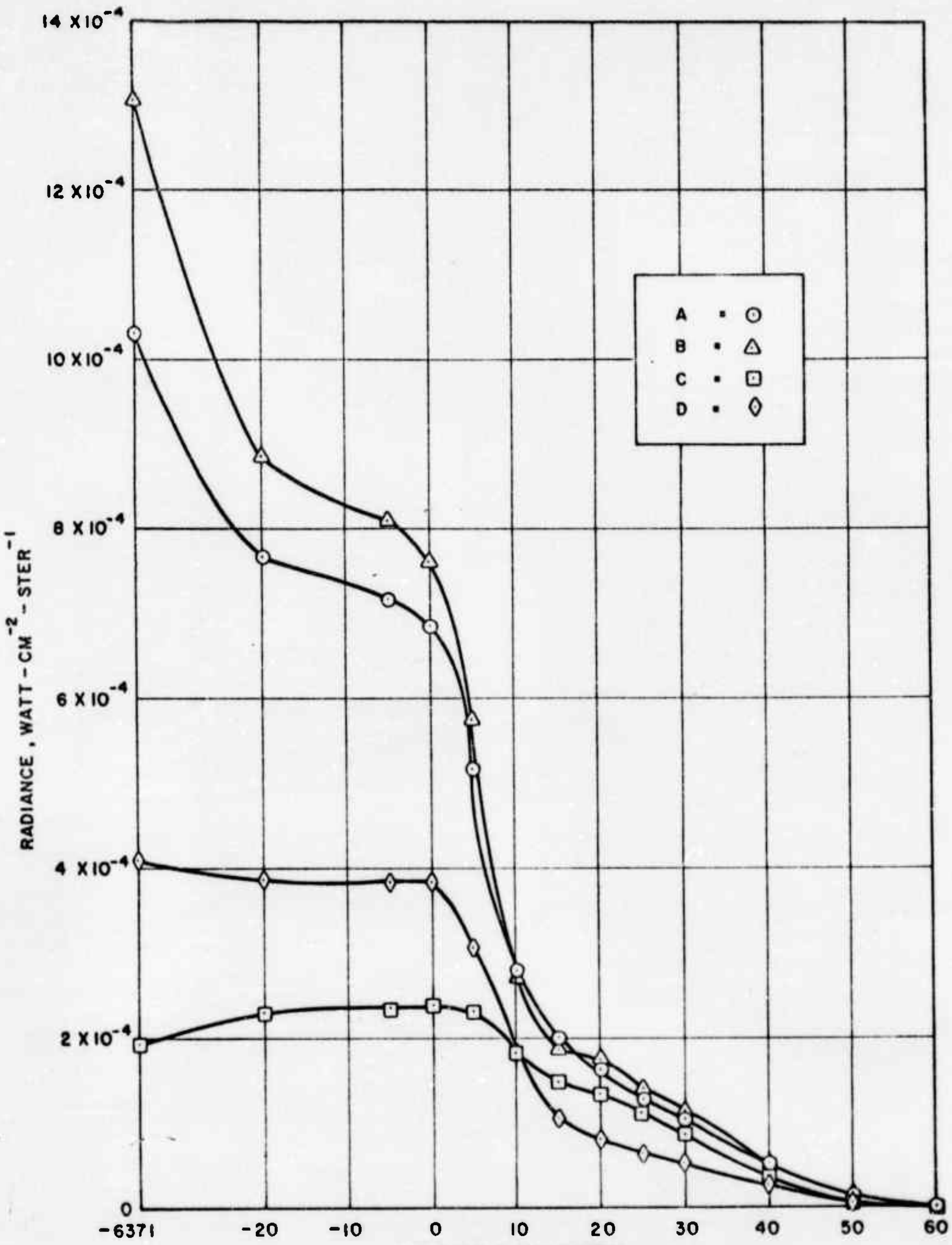


Figure 6. Atmospheric Models A, B, C, and D (Radiance Vs Altitude, 12.30 to 14.80 Microns)

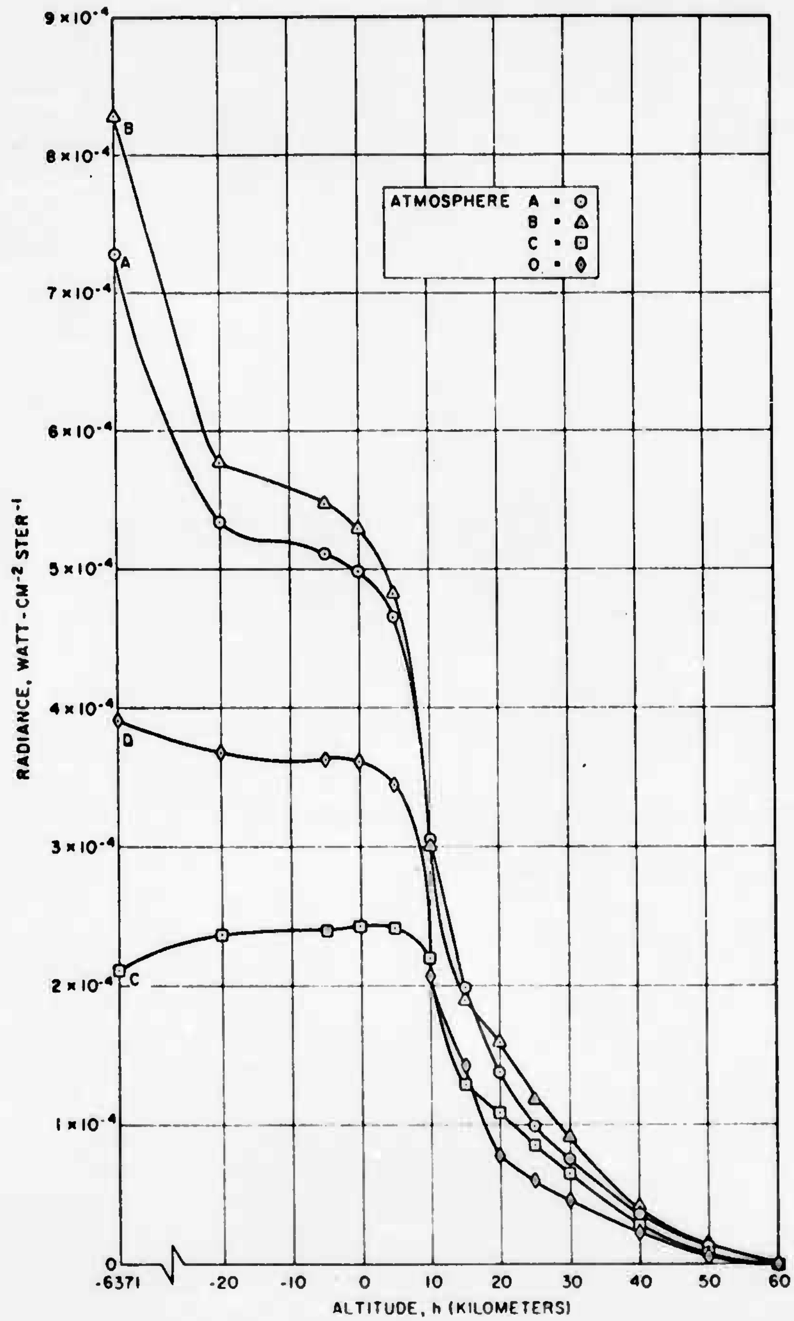


Figure 7. Atmospheric Models A, B, C, and D (Radiance Vs Altitude, 16.0 to 18.2 Microns)

## IV. "TWO COLOR" HORIZON SENSING TECHNIQUE

Another possible horizon sensing technique is the use of a "two color" horizon sensor.[1] This would involve the use of two detectors mounted on the same substrate, equipped with individual filters transmitting in slightly different spectral regions. The electrical output of one detector would be subtracted from that of the other and the difference signal would be used in determining the position of the horizon.

Following is a brief explanation of the principle involved in this technique. It will be assumed that one of the two spectral regions selected is located at the center of the $CO_2$ absorption band (let this be called band a), while the other spectral band (let this be called band b) of approximately the same width is located just to the long or short wavelength side of band a. As the line of sight of the horizon sensor moves into the earth's atmosphere, the radiance in band a will be somewhat higher than that in band b, since the absorption, and hence the emissivity, is greater for band a than for band b. This radiance difference will increase for a time as the line of sight moves deeper into the atmosphere. Since the atmosphere is more transparent for band b than for band a, eventually a point will be reached where the radiance in band b will increase at a greater rate than in band a, since the radiation in band b by this time originates from regions deeper in the atmosphere where the temperature is greater. Thus the two radiance curves will come closer together, or even cross. At some point, a maximum difference in radiance occurs. The position of this maximum should have a reasonably well defined location with respect to h, the minimum altitude of the line of sight.

Figure 8 shows radiance curves for atmosphere A for the two spectral regions; 14.29 to 16.0 microns and 16.0 to 17.4 microns, plotted against h. Also shown is a curve representing the difference between these curves. The difference curve in this case reaches a maximum at h = 27 kilometers.

---

[1] This technique was first suggested by John Duncan of the University of Michigan.

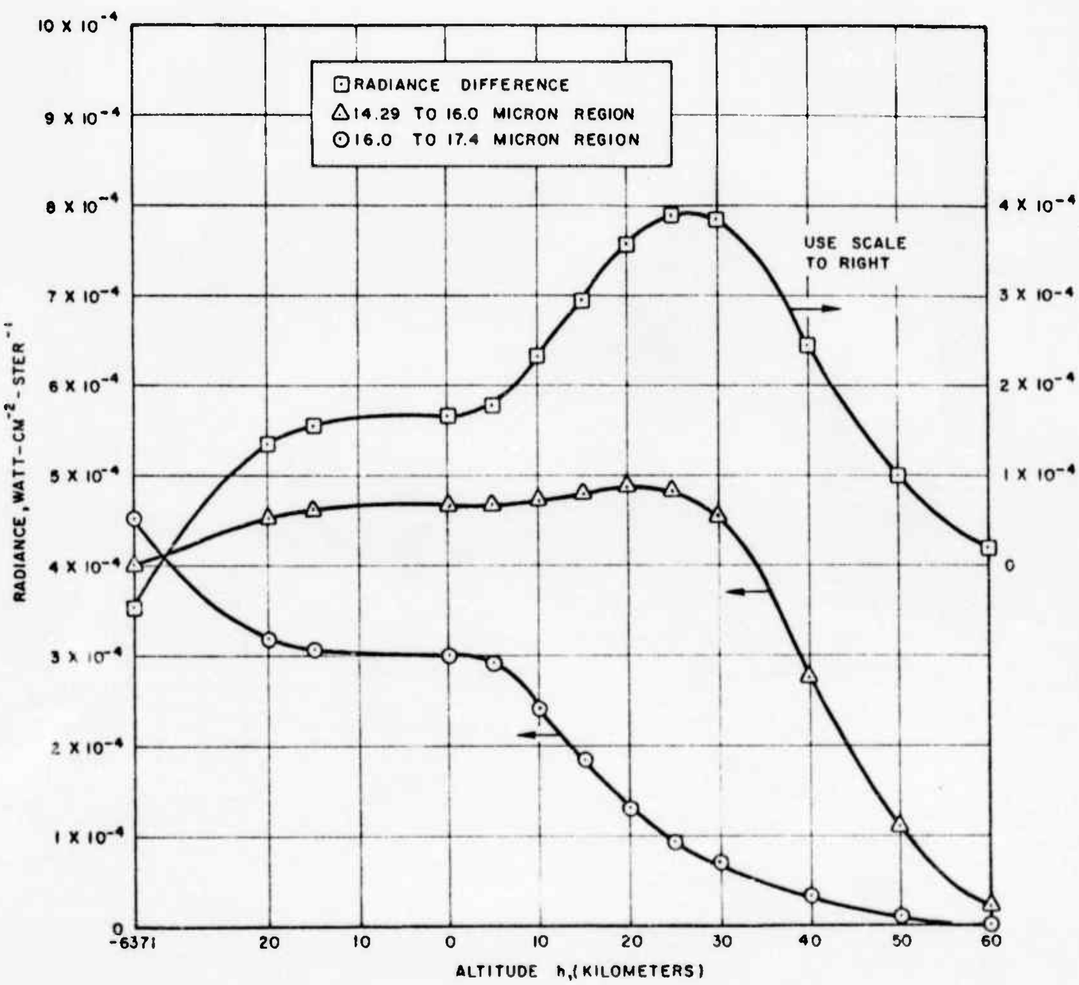


Figure 8. Atmospheric Model A (Radiance and Radiance Difference Vs Altitude, 14.29 to 16.0 and 16.0 to 17.4 Microns)

Corresponding curves for atmosphere C are shown in Figure 9. Table 3 shows the positions of the peaks obtained using each of the atmospheric models.

Table 3. "Two-Color" Horizon Sensing Technique

| Atmospheric Model | Altitude of Max. Difference in km for 14.29 to 16.0 μ and 16.0 to 17.4 μ Bands | Altitude of Max. Difference in km for 14.29 to 16.0 μ and 12.85 to 14.29 μ Bands |
|---|---|---|
| A | 27.0 | 27.5 |
| B | 25.0 | 25.0 |
| C | 24.0 | 24.0 |
| D | 26.0 | 24.0 |
| E | 25.0 | 26.0 |
| F | 25.5 | 25.0 |
| G | 25.8 | 25.0 |
| H | 25.0 | 25.0 |
| Maximum Spread (km) | 3.0 | 3.5 |
| Standard Deviation ($\sigma$) | .83 | 1.06 |

The maximum difference is 3 kilometers and the standard deviation is 0.83. The position of this peak as a criterion for defining the horizon appears to be as good as or better than the normalization method mentioned earlier. However, it does have two important disadvantages over the normalization method. One is the greater complexity required in the horizon sensor, particularly in the electronics; the other is that it would probably be more difficult to detect the exact position of the maximum (where the slope is zero) than it would be to measure the horizon at a fixed percentage of the maximum radiance.

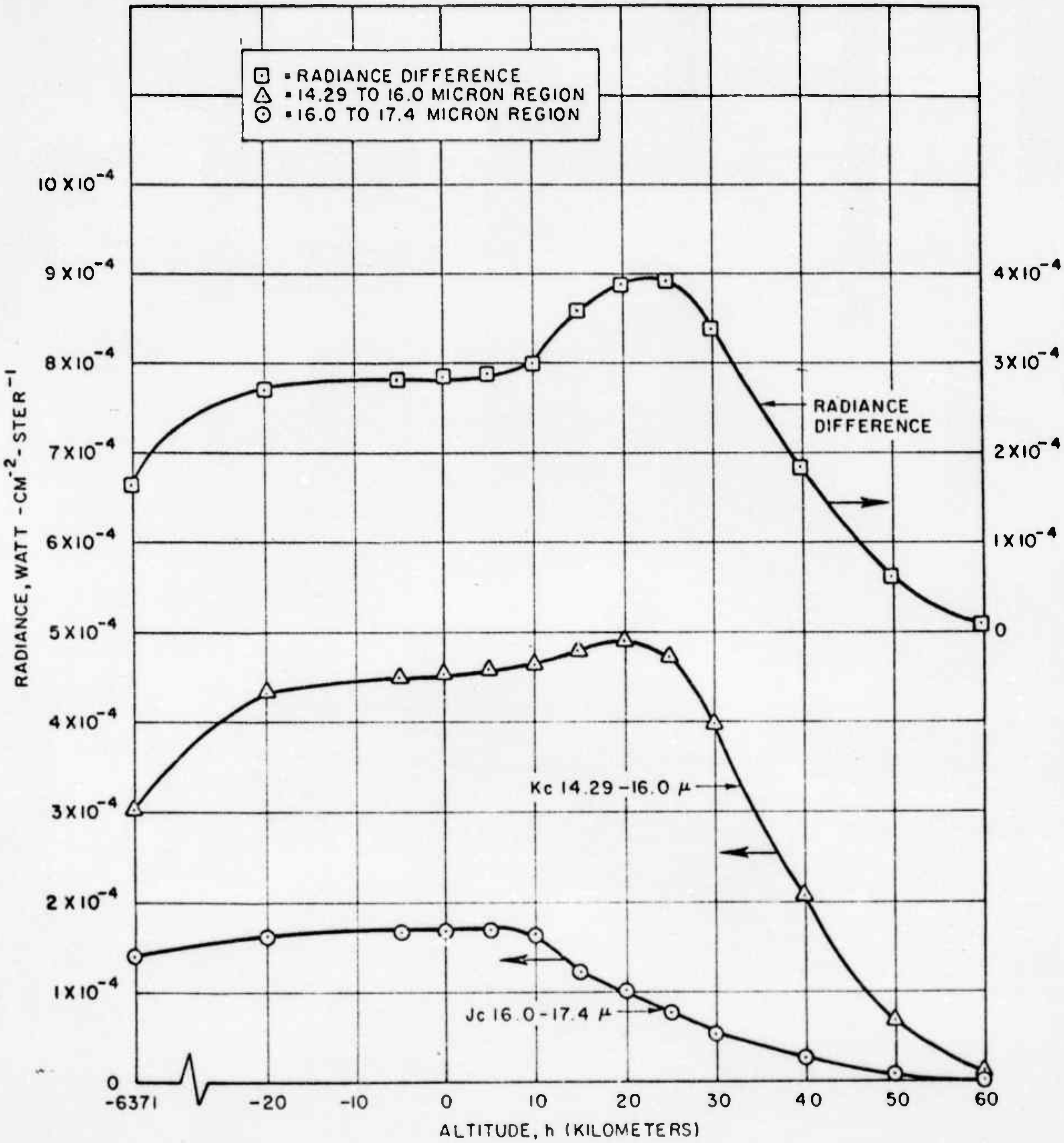


Figure 9. Atmospheric Model C (Radiance and Radiance Difference Vs Altitude, 14.29 to 16.0 and 16.0 to 17.4 Microns)

Figures 10 and 11 show the same type of curves for atmospheres A and C for the 14.29 to 16.0 micron and the 12.85 to 14.29 micron regions. Table 3 also shows the position of the peak difference for each of the atmospheric models for these spectral bands. Here, the maximum difference and the standard deviation are somewhat greater than for the case previously considered. The 12.85 to 14.29 micron band is partially in the 8 to 13 micron atmospheric window, where one would expect the variations to be greater.

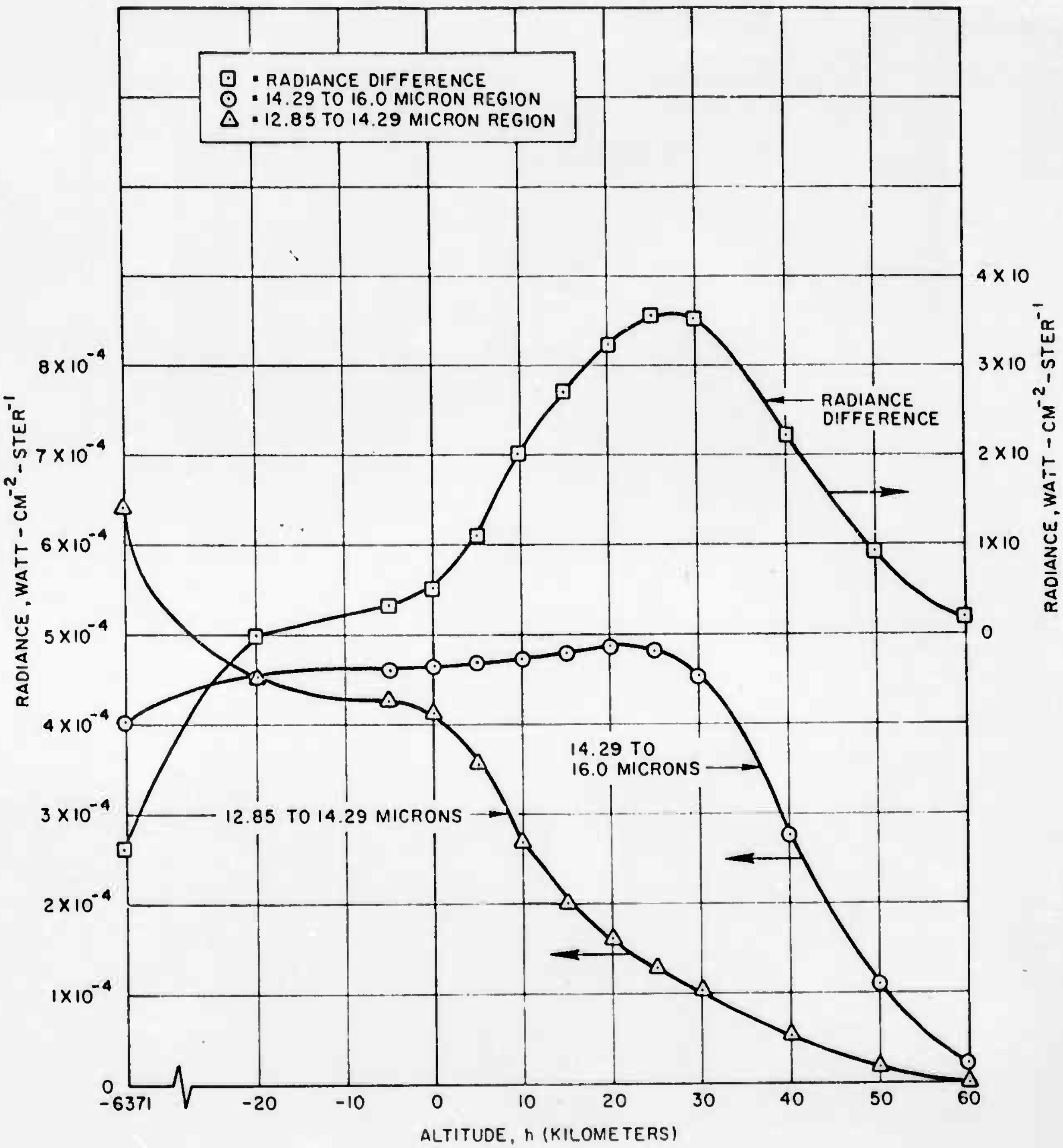


Figure 10. Atmospheric Model A (Radiance and Radiance Difference Vs Altitude, 14.29 to 16.0 and 12.85 to 14.29 Microns)

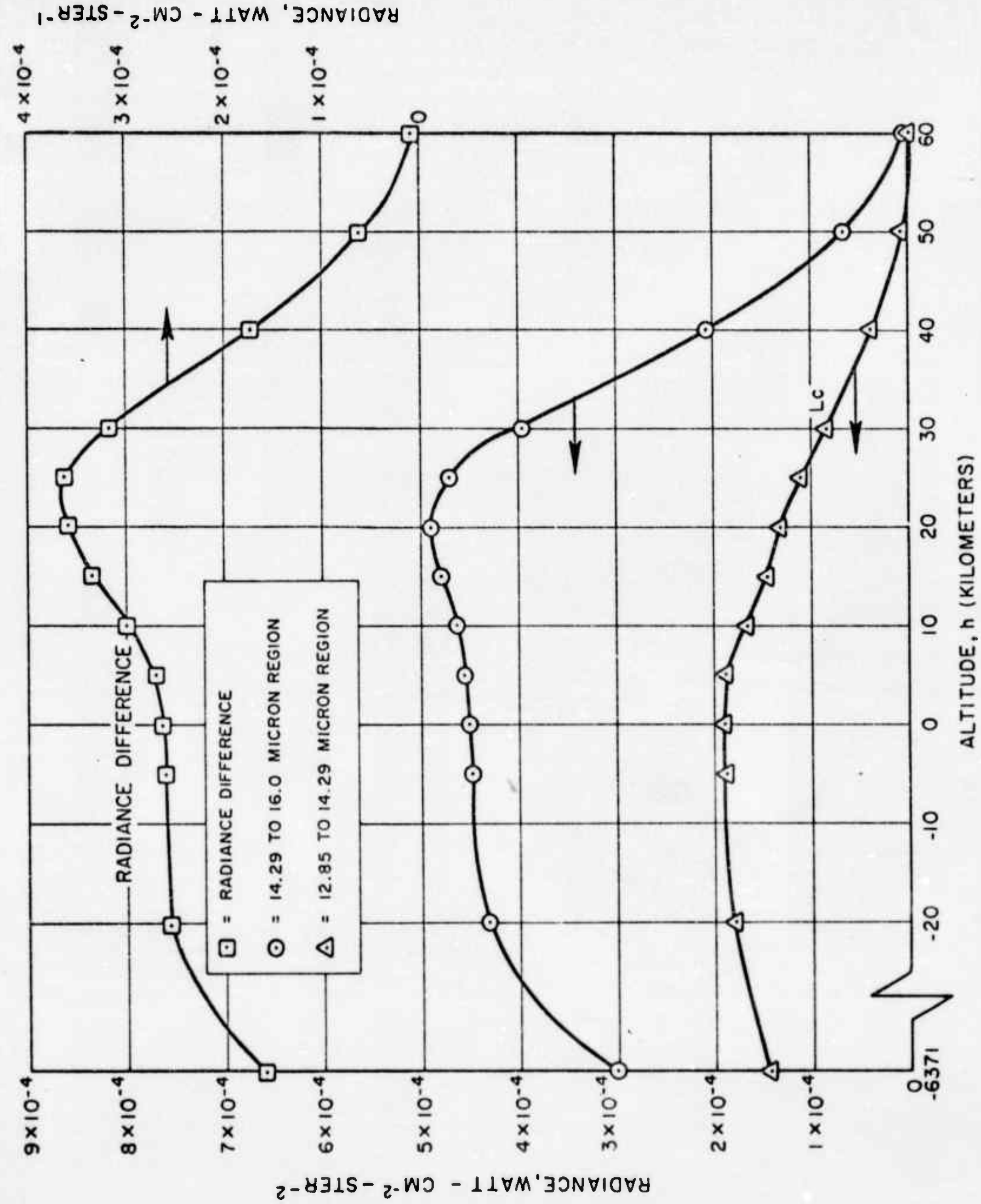


Figure 11. Atmospheric Model C (Radiance and Radiance Difference Vs Altitude, 14.29 to 16.0 and 12.85 to 14.29 Microns)

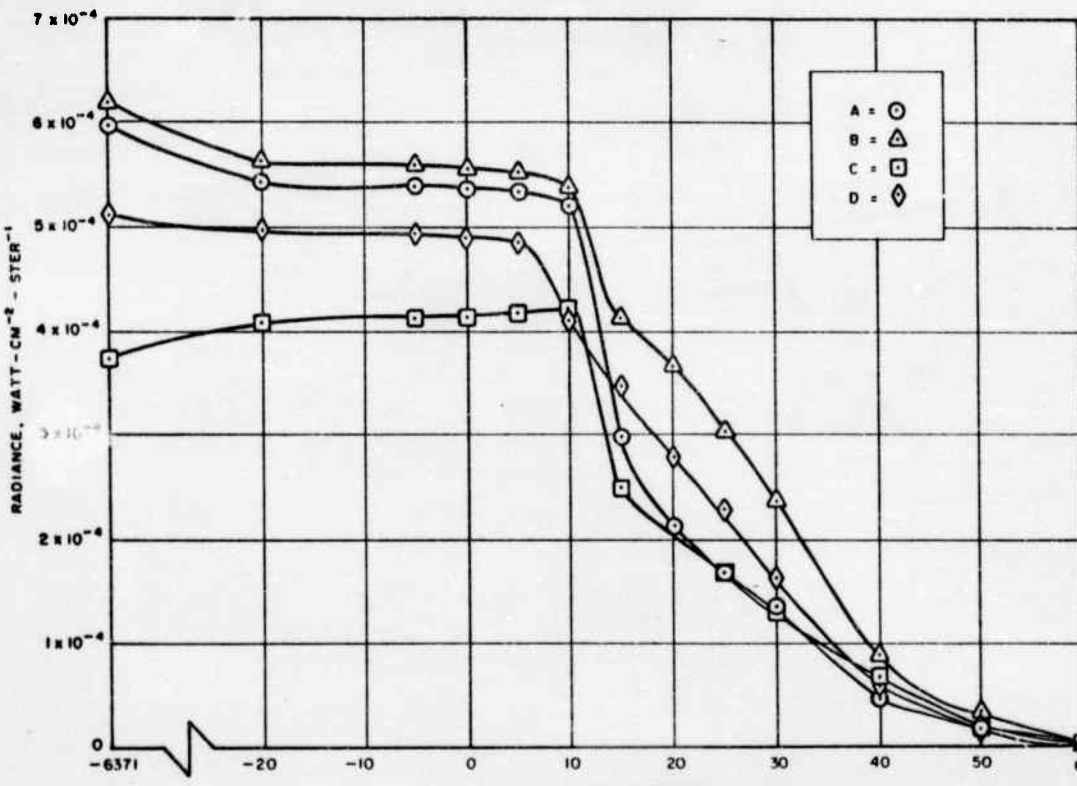


Figure 12. Atmospheric Models A, B, C, and D (Radiance Vs Altitude, 28.6 to 40.0 Microns)

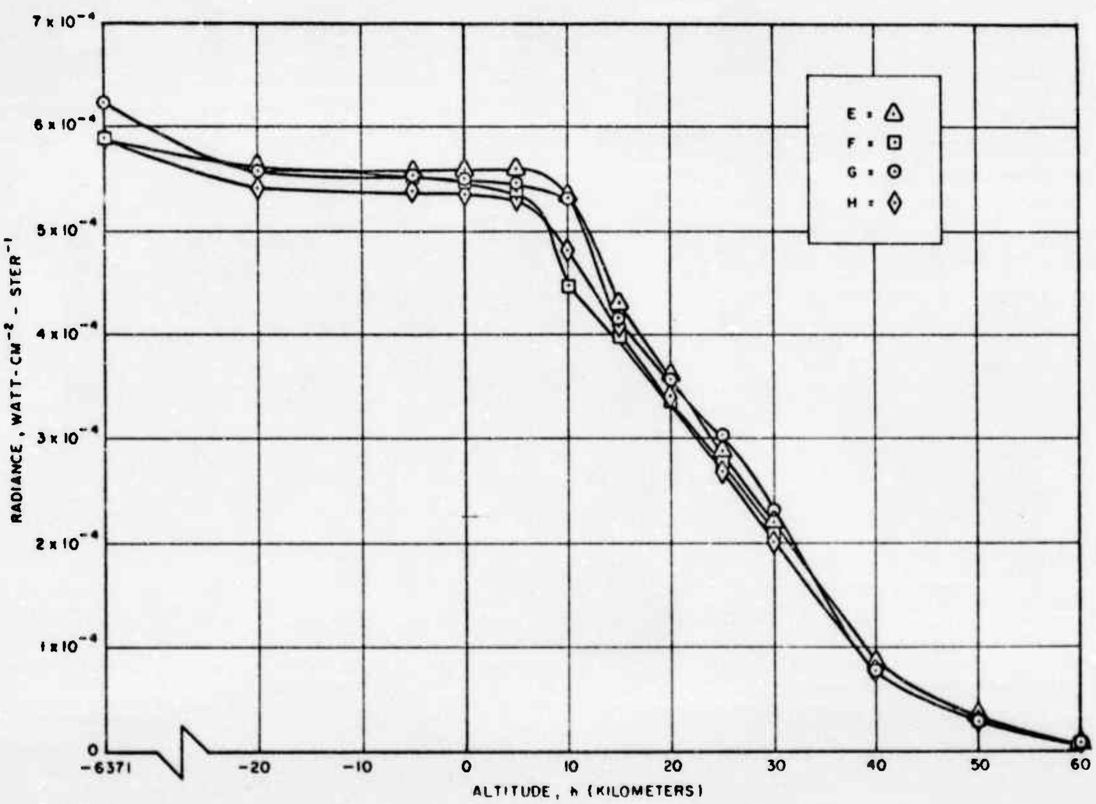


Figure 13. Atmospheric Models E, F, G, and H (Radiance Vs Altitude, 28.6 to 40.0 Microns)

## V. THE LONG WAVELENGTH ROTATIONAL ABSORPTION BAND OF WATER VAPOR

Figures 12 and 13 show atmospheric radiance versus altitude for the 28.6 to 40.0 micron spectral region. This region is within the broad rotational absorption band of water vapor.

These curves, particularly those of Figure 12, show more variation in shape than those showing the radiance in the 14.29 to 16.0 micron region. Table 4 shows the values of altitude resulting if the arbitrary position of the horizon is assumed to be at the 50 percent point on each of the radiance curves. The extreme difference, occurring between atmospheres A and G, is 11.5 kilometers. When a standard deviation is computed from this set of values, its value is found to be 4.78 kilometers. The limited data available thus indicate that this spectral region is inferior to the 15 micron $CO_2$ region for use in horizon sensing.

Table 4. Analysis of Horizon Radiance Data for 28.6 to 40.0 Micron Spectral Region

| Atmospheric Model | Altitude in km Corresponding to 50% Radiance Point |
|---|---|
| A | 16.0 |
| B | 27.0 |
| C | 18.0 |
| D | 22.5 |
| E | 25.5 |
| F | 25.5 |
| G | 27.5 |
| H | 25.0 |
| Maximum Spread in km | 11.5 |
| Standard Deviation ($\sigma$) in km | 4.78 |

The large variations that occur in the horizon radiance profile in the water vapor absorption band are largely caused by the nonuniformity of distribution of water vapor in the atmosphere as compared to carbon dioxide. Another disadvantage involved in the use of the 30 to 40 micron region for use in horizon sensing is the difficulty of obtaining suitable optical materials in this spectral region. This disadvantage alone, however, would not be an unsurmountable one.

## VI. CONCLUSIONS

The graphs shown in this report, together with the data on which they are based, show that a reasonably narrow spectral region centered at the 15 micron carbon dioxide atmospheric absorption band appears to be the best region in which to operate an infrared horizon sensor. The results show that it may be possible with proper mechanization to achieve 1$\sigma$ uncertainties as small as 0.9 to 1.3 kilometers in altitude when determining the direction of the line of sight from a space vehicle to the apparent horizon.

If the vehicle is assumed to be located at an altitude of 100 nautical miles, this error in distance would correspond to an angular 1$\sigma$ error of less than 0.05 deg.

It was also determined that, if the $CO_2$ absorption region is used in horizon sensing, the selected spectral region should not only be as narrow as is consistent with signal-to-noise requirements, but should also be located at the center of the absorption band.

A "two color" horizon sensing technique, in which the maximum difference in radiance between two adjacent spectral regions is used as the criterion for establishing the position of the line of sight to the horizon, has been described. It has been shown that this technique can achieve accuracies comparable to those of the more conventional technique described earlier. However, the two color technique involves more difficulty in mechanization and in data processing.

The spectral region from 28.6 to 40.0 microns contained within the rotational water vapor absorption band is shown to be considerably inferior to the 14.29 to 16.0 micron region for horizon sensing purposes. An additional disadvantage of using this water vapor absorption band is the scarcity of suitable optical materials for this spectral region.

The effects of spectral filters, which would, of course, be required in any actual system to isolate the observed wavelength regions, has not been considered in this report. However, no serious problems are contemplated

here. Some variation in the actual cut-on and cut-off wavelengths of the filters can be tolerated without seriously degrading the system.

The most important factor in selecting the filter is to have very high rejection of radiation at wavelengths appreciably outside the selected limits. Present filter manufacturing techniques are sufficient to produce filters of the required accuracy.

The attenuation of the signal by the filter is not expected to be serious in the $CO_2$ absorption region. For example, filters for the 14.29 to 16.0 micron region can be produced having a peak transmission of between 20 and 40 percent.

The problem is somewhat worse in the water vapor absorption region, where a filter for the 28.6 to 40.0 micron spectrum region would probably have a maximum transmission of about 10 percent. Since there is considerable energy in this band, the filter will not present an insurmountable problem.

This report attempts to give an estimate of the accuracy which might be expected of infrared horizon sensors operating in the long wavelength atmospheric absorption bands. Much more data covering a wider variety of seasonal, geographical, and diurnal conditions, are needed before final conclusions can be reached. It is planned to publish additional reports, analyzing further data as they become available.

## REFERENCES


1. Ehlers, Donald E., "Temperature Measurement of Earth and Clouds from a Satellite," paper presented at the Second Symposium on Remote Sensing Environment, University of Michigan, Ann Arbor, Michigan, October 15-17, 1962

2. Hanel, R. A. et. al. "The Infrared Horizon of the Planet Earth," J. of the Atmospheric Sciences, Vol 20, No. 2, March 1963

3. Eastman Kodak Company, "Measurement of 15-Micron Horizon Radiance from a Satellite," Contract AF 04(695)-160 EK/ARD ED-995, for SSD, USAF, submitted by Apparatus and Optical Division, Lincoln Plant, Rochester, N. Y., March 1, 1963

4. L. Bradfield, "Horizon Sensor Infra-Red Flight Test Program," Lockheed Missiles and Space Company, Sunnyvale, California, Rept. No. A064189, 19 October 1962

5. D. Q. Wark, et. al, "Meteorological Satellite Laboratory Report No. 21, Calculations of the Earth's Spectral Radiance for Large Zenith Angles," U. S. Dept of Commerce, Weather Bureau, Washington, D. C.

DISTRIBUTION

Internal

M. D. Earle
L. Hirschl
M. Jensen
S. Konopken
W. Leverton
I. G. Lowe
D. McColl
C. L. Patterson
A. G. Nash
F. Sabin
R. W. Slocum
E. B. Soltwedel
J. C. Travis

External

Maj W. T. Jones
SSZA

Maj E. A. Lembeck
SSVA

Capt E. De Avies
SSTRT

J. Dodgen
National Aeronautics
and Space Administration
Langley Research Center
Langley Field, Va.

D. Q. Wark
U.S. Weather Bureau
Suitland, Md.

John Duncan
University of Michigan
Ann Arbor, Michigan

J. Heiatt
Space Technology Laboratories
One Space Park
Redondo Beach, Calif.

A. Koso
Instrumentation Laboratory
Massachusetts Institute of
Technology
Cambridge, Mass.

E. Wormser
Barnes Engineering Company
Stamford, Conn.

Tom Shiell
Advanced Technology Laboratories
369 Whisman Road
Mountain View, California